CHAPTER 5

Electronic Properties of Wells–Dawson Anions

Together with the Keggin anion, studied in previous chapters, the Wells–Dawson molecule is, probably, the second heteropolyanion in popularity. Its structure is somewhat larger and, in general, can be formulated as $X_2M_{18}O_{62}^{n-}$. Some similarities are visible in the shape of Keggin and Wells–Dawson anions. In spite to this, some properties are different, indeed. The main goal of this chapter is to describe, in a systematic way, the geometry and electronic properties related to the structure, and they are compared with regard to the Keggin anion. The redox properties are studied in relation to the electronic structure. Both single- and mixed-addenda compounds are studied and compared for finding general rules of chemical behaviour. The last part of the chapter is devoted to the isomerism. Three isomeric forms are known for the Wells–Dawson anion: α, β and γ. We will focus the attention of the reader in the first two, the most commonly studied, showing what are the major differences compared to Keggin anions. So, the relative stability of the α/β pairs is examined as well as the changes introduced in the reduction potential as we vary the shape or the chemical composition.

5.1. Electronic Structure of α-Wells–Dawson Anions

Fully oxidised structures

We have seen in Chapter 4 that the most common structure amongst all the heteropolyanions, the Keggin structure, has twelve equivalent metal centres in its α form, which confers the experimentally observed T_d symmetry to the framework. A. F. Wells[1] in the middle 40's first postulated the structure for the α-$P_2W_{18}O_{62}^{6-}$ anion. In 1953, Dawson reported the first (low-resolution) X-ray experiment for the same anion,[2] whereas Strandberg[3] and D'Amour[4] later reported more accurately results to determine the structure, now formulated in general as $X_2M_{18}O_{62}^{n-}$. Those reports did not confer full equivalence to the eighteen metal centres, so a distinction was made between polar (α_2 positions or *caps*) and equatorial regions (α_1 positions or *belts*). The two polar fragments are composed of three edge-sharing octahedra (triads), whereas the equatorial M_{12} array is formed via alternative corner- and edge-sharing MO_6 units, as displayed in Figure 5.1.

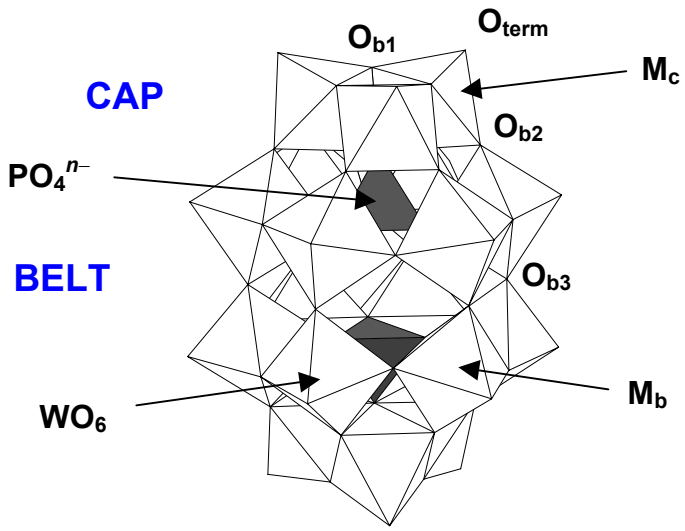

Figure 5.1. Polyhedral representation of the α-$P_2W_{18}O_{62}^{6-}$ Wells–Dawson anion. Two identical fragments or hemispheres are easily identifiable, each composed of one capping triad and one equatorial belt with six WO_6 octahedra. Relevant positions are labelled for further discussion.

Each of the equatorial octahedra is connected to a polar octahedron by a single corner and it shares one edge with a neighbour of the same belt and a corner to the other belt. Two $XO_4^{(n/2)-}$ units are encapsulated inside the formally neutral $M_{18}O_{54}$ cage,[5] containing the greater part of the negative charge of the POM. The structural characterisation of the WD anion is compatible with a D_{3h} point group of symmetry. From the information provided here concerning the nature of the assembly of the octahedra in the WD framework, not only a geometrical distinction but a chemical one can be made for the two different regions of the structure

The WD derivative is may be seen as a derivative of the Keggin structure as follows. The removal of three neighbouring corner-sharing octahedra in, say, α-PW_{12}, produces a lacunary structure, formulated as A-α-PW_9, which is ready to join another equivalent moiety to produce the α-P_2W_{18} assembly (Figure 5.2). ESR and electrochemical studies[6] have shown that WD anions are chemically different compared to the Keggin species in some aspects. To be more concrete, it has been shown that the localisation of extra electrons (metallic electrons) does not obey a strict balanced sharing but there are preferential sites for the trapping of these electrons, differently from the single-addenda α-Keggin case. An explanation to this phenomenon is found in the geometric parameters that make the Keggin and the WD forms different. In this section we will deal only with single-addenda WD structures, introducing the general features like the electronic structure and related properties.

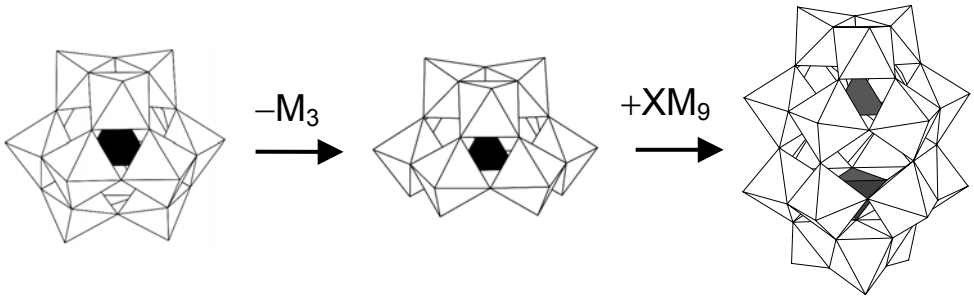

Figure 5.2. Polyhedral representation of the α-XM_{12} Keggin anion, the A-XM_9 lacunary anion derived by removing 3 corner-sharing octahedra, and the Wells–Dawson structure X_2M_{18}, formed by adding an M'$_3$ or another A-XM_9 unit, respectively.

Some structural parameters in WD anions are special. We highlight the M–O–M angle between corner-sharing octahedra of the two belts in the equatorial region. It was computed at the DFT level, being 163º in both P_2W_{18} and P_2Mo_{18} cases. The experimentally measured value is fairly close to that, about 162º.[3] The corresponding M–O–M angle in the cap is close to 125º, the typical value of edge-sharing Keggin-like triads. So, almost linear M–O–M angles appear linking the two halves of the anion and this fact has serious implications in the chemistry of the WD molecule. One of them is

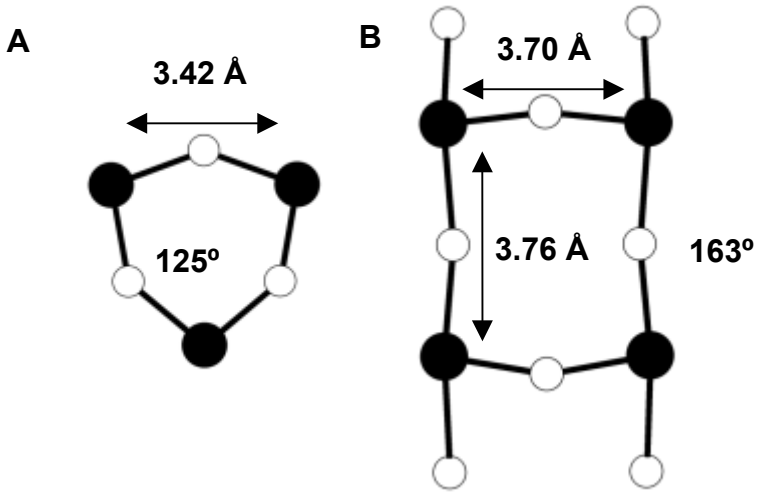

Figure 5.3. Relevant distances and angles for the P_2W_{18} Wells–Dawson anion (black circles–tungsten, white circles–oxygen). In A only metal atoms and bridging oxygens of a polar triad are represented. In B, a part of the equatorial region is shown. Of the four metal atoms represented, those separated by 3.70 Å belong to the same belt, whereas the separation of 3.76 Å is between the two belts.

that metal centres are much more separated, in average by 3.7–3.8 Å, than in polar regions, where the distance between two neighbouring metals is ~3.4 Å, the typical distance in Keggin forms. In the caps, edge-sharing octahedra imply smaller MOM angles and shorter M–M distances (Figure 5.3), whereas in the belt regions, octahedra linked by corners allow metal centres to be farther, and, in addition, MOM angles are bigger. The other structural parameters are somehow common to all the heteropolyanions. In tungstates, all the W=O (terminal) bond lengths were computed to be ~1.74 Å, a value

that is very similar to the W=O distance found for XW_{12} structures[7–8] and it is 0.05 Å longer than the experimental distance. The W–O (bridge) distances are also similar to those found in Keggin anions. They are about 1.90–1.94 Å in the tungstate. In principle, the error introduced in the terminal distances may not alter the reduction properties discussed here since they essentially would affect to the d_{xz}- and d_{yz}-type orbitals that are not involved in the most common reduction processes of these species[8] (see chapter 3). This is so since they do not contribute to the lowest unoccupied MOs. We will see below that some new considerations have to be discussed for the case of 2:18 molybdates.

Table 5.1. Percentile contributions of belt and cap metal centres to the LUMO, LUMO+1 and LUMO+2 for single-addenda WD anions.

Anion	*Sym*	*Belt*	*Cap*	*Belt*	*Cap*	*Belt*	*Cap*
		a_1”		e”		e’	
P_2W_{18}	D_{3h}	70	0.5	61	10	20	48
P_2Mo_{18}	D_{3h}	62	1	54	9	22	40

A deeper analysis of the MO structure of WD anions shows the typical arrangement found in most of the heteropolyanions containing only early transition metals, where the oxo band and the empty set of d_{xy}-metal orbitals are perfectly separated. For comparison, Figure 5.4 contains an energy diagram for the lowest unoccupied orbitals of 1:12 and 2:18 tungstates and the 2:18 molybdate. It is worth noting that the relative energy of the unoccupied set of orbitals is lower in the case of WD anions, compared to the Keggin form displayed. Table 5.1 gives percentile metal contributions to the LUMO, LUMO+1 and LUMO+2 for idealised D_{3h} P_2W_{18} and P_2Mo_{18} structures. All these unoccupied orbitals are formally symmetry adapted d_{xy}-tungsten orbitals with some antibonding participation of the oxygen orbitals (Figure 5.5). Under the constraints of the D_{3h} point group, the symmetries of the first three unoccupied orbitals are a_1”, e” and e’, respectively. The contribution of cap and belt metals to these three orbitals is unequal; the d_{xy}-orbitals centred on the belt metals are the major contributors to the LUMO and LUMO +1. When the energy of the orbital increases the participation of the cap-centred atomic orbitals also increases (from, ~1% in the LUMO to

~48% in the LUMO+2 in the tungstate and to ~40% in the molybdate). A 3D representation of the a_1" orbital (Figure 5.5) shows that the LUMO is only localised over the *belt* tungstens. It should be pointed out that this orbital appears at 2.25 eV above the occupied oxo band, 0.55 eV lower than the relative energy of the degenerate LUMO of e symmetry in PW_{12}. The metal orbitals in PW_{12} and P_2W_{18} have an antibonding character between the metal and oxygen orbitals but also between two adjacent metals. The M–M antibonding interaction is lower when the two adjacent metals belong to two different PW_9 moieties (the metal-metal distances are longer) and therefore the d_{xy}-type orbitals delocalised among the equatorial tungstens have lower energies than the corresponding orbitals in the Keggin structure.

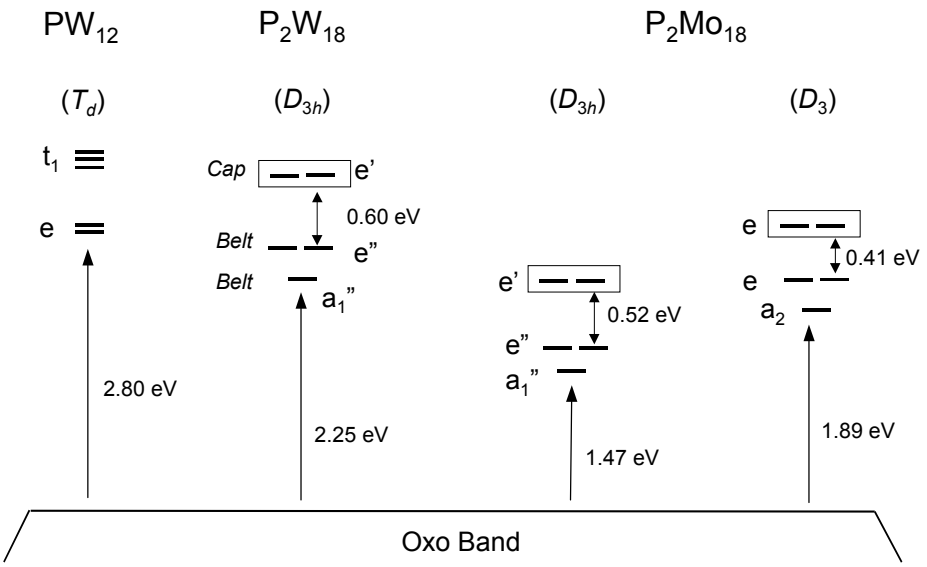

Figure 5.4. Molecular orbitals scheme for the α-PW_{12} anion and the single-addenda WD heteropolyanions with M = W and Mo. In the latter case, we show the orbitals associated to the D_{3h} and D_3 structures. The orbitals in frames are those localised on the polar triads of the corresponding WD structures.

Let us introduce here the case of the molybdate anion. It is well known from experiments that heteropolyanions in general, and 2:18 molybdates in particular, have a very characteristic structure. In fact heteropolymolybdates

in general. Whereas the α-P_2W_{18} anion possesses D_{3h} symmetry, the homologous molybdate is formed of three interpenetrating loops of alternately long and short Mo–O bonds, therefore the structure is distorted. This phenomenon confers chirality to the anion, the symmetry of which is D_3. Experimental evidence of the chirality was obtained from X-ray data,[3-4] ^{17}O NMR,[9] IR spectroscopy and optical rotatory dispersion[10-11] measurements. Both symmetric and distorted geometries were computed at the DFT level for the 2:18 molybdate anion. The bridging Mo–O bonds computed for the D_3 geometry range between

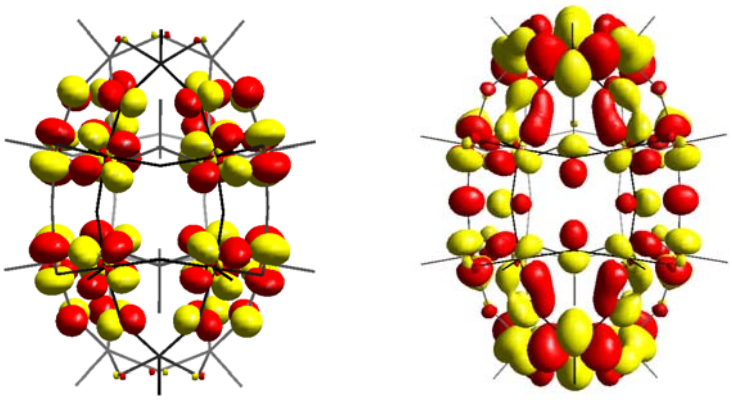

Figure 5.5. It is showed a 3D representation of the LUMO and LUMO+2 (one component) of α-P_2W_{18}. The first one is clearly localised on the equatorial centres, whereas the major contribution of the second orbital comes from the polar regions.

1.84 and 2.12 Å,[12] distances in close agreement with the X-ray data available (1.8–2.1 Å). On the other hand, the Mo=O_{term} distances and all the angles are very close to those of the tungstate anion. The D_{3h}-idealised, highly-symmetric α structure has a LUMO 1.47 eV above the oxo band, an energy that represents again a decrease of 0.56 eV with respect to the H-L gap in PMo_{12}. The equatorial belts maintain the traditional Mo–O distances, of about 1.9 Å. The lowering of the symmetry from D_{3h} to D_3 is accompanied by a considerable stabilisation of 0.32 eV (>7 kcal mol^{-1}) and an enlargement of the H-L gap to 1.89 eV. This value is quite close to the

energy gap of 2.03 eV found for the idealised T_d form of α-PMo_{12}.[8] So, in general, the transformation of a PM_{12} into a P_2M_{18} decreases the H-L gap more in tungstates than in molybdates.

Reduced single-addenda structures

The redox properties of a given molecule are intimately related to the energy and composition of the LUMO. According to the orbital diagram in Figure 5.4, the first reduction in P_2W_{18} and P_2Mo_{18} must take place in the *belt* region. After the exploration of the electronic structure of fully oxidised POMs we can explicitly reduce the clusters to get more precise information about the localisation of the metal electrons and the energy required for carrying out the reductions. Calculations conducted on the reduced structures confirmed the hypothesis that equatorial metals would accept extra electron first, and the ground state for the single reduced P_2W_{18} is a $^2A_1$" with 98% of the spin density localised over the belt metals (Table 5.2).

Table 5.2. Spin polarisation (α – β) and relative energies (in eV) for the first three lowest states in several single-addenda reduced WD Anions.

	Sym	(α – β)		*E*	(α – β)		*E*	(α – β)		*E*
		$^2A_1$			^2E"			^2E'		
		Belt	Cap		Belt	Cap		Belt	Cap	
P_2W_{18}	D_{3h}	0.98	–0.03	0.00	0.87	0.13	0.30	0.26	0.69	0.84
P_2Mo_{18}	D_{3h}	0.89	–0.05	0.00	0.83	0.14	0.20	0.27	0.66	0.69

The first excited state (^2E") has the spin density essentially localised over the belt metal centres (87%) and lies at about 0.30 eV above the ground state. The reduction in the cap sites requires about 0.84 eV more than the ground-state reduction; it involves the addition of one electron to the LUMO+2 (e'). In that case, the associated state is ^2E'. The term ^2E' is characterised by having 0.69 alpha electrons delocalised among the six cap tungsten atoms and 0.26 e among the twelve belt-centres. For the analogous molybdate, the energy associated to the belt ($^2A_1$") and cap (^2E') reductions differs by 0.69 eV for the D_{3h} isomer (exactly the energy gap between the LUMO and the LUMO+2). In the D_3 form, the separation between these

MOs is the same, which suggests that the energy difference between both site reductions should be very close to the value obtained for the D_{3h} form. All these results fully agree with the experimental data of Pope[6b] and Contant[22] who demonstrated that equatorial sites are more easily reduced than polar sites. These values of spin polarisation and electron localisation are in fair accordance with the study of the electronic structure of oxidised clusters, which is the proof that a simple MO analysis is a good approximation to study the features of the reduced molecule.

Calculations carried out for α-P_2W_{18} of symmetry D_{3h} showed that the reduction at the cap sites –addition of one electron to the LUMO+2 (e')– requires 0.84 eV more than the reduction at the belt sites –addition of one electron to the LUMO (a_1").[12] The spin polarisation data confirm that the first metallic electron is delocalised over the *belt* metal centres. For the two-fold-reduced species, both the high- and low-spin electronic configurations were computed. In α-P_2W_{18}, the closed-shell configuration $(a_1")^2$ $(e")^0$ (see Figure 5.10) was found to be 4.0 kcal mol^{-1} more stable than the triplet state $(a_1")^1$ $(e")^1$, which was determined allowing Jahn–Teller relaxation. These results agree with the lack of ESR signal for the two-electron-reduced species.[6c] It is well established that Keggin anions and related structures with an even number of delocalised electrons have a diamagnetic behaviour. Although it was initially attributed to a strong antiferromagnetic coupling via a multiroute superexchange mechanism,[13] recent theoretical studies have shown that electron repulsion and electron delocalization can also stabilise the singlet ground state.[14-16] The theoretical analysis of the coupling of delocalised electrons is a sophisticate problem that, in the case of large systems like POMs, will still need some time to have concluding results.

We can associate now all the features exposed above with the particular structure of WD anions. We saw at the beginning of the chapter what are the main structural differences between P_2M_{18} and PM_{12} molecules. These are centred in the equatorial region, where almost linear M–O–M linkages unite the two belts. First, the antibonding interactions between neighbouring metals from different belts are less effective since they are, in average, 0.3 Å further from each other compared to the M–M distance in a polar triad. Second, there is no contribution of the bridging oxygens (O_{b3}) in this region. Only antibonding interactions appear between belt metals and O_{b2} sites. Neither between belt metals and belt oxygens an antibonding overlapping occurs since there are symmetry restrictions that forbid the p-O_{b3} orbitals to

contribute to the LUMO. Therefore, only a few antibonding p(O)-d(M) interactions appear in the LUMO, and the overall balance for this property allows this MO to be very low in energy.

5.2. Effect of the Chemical Substitution on the Redox Properties of α-Wells–Dawson Anions

After exposing in detail the characteristics of the WD anions with only one type of addenda metal, we can face now the study of more complex clusters, not from a geometrical point of view but concerning the chemical composition. The region of frontier orbitals of a given α-X_2M_{18} anion follows a unique rule; the LUMO and LUMO+1 are composed, nearly exclusively, by contributions of the valence d orbitals centred in the *equatorial* metals plus some contribution of bridging-oxygen p orbitals (see representation in Figure 5.5). On the other hand, the first unoccupied MO localised on the cap octahedra is considerably high in energy. In this section we explore the effect of combining different elements in the same framework, dealing with the most common early transition-metal elements appearing in POMs: W, Mo, V and Nb. The main goal is to describe the MOs of suitable $P_2M_{15}M'_3$ anions and to study their redox properties by means of the knowledge of the electronic structure. In this representation, the three M' centres are all located in the same cap, thus sharing edges. It is expected that the most important changes are introduced in this region, and that a modest influence spreads to other parts of the framework. The principal change in the electronic structure of the WD anion we can think of is one in which the single-addenda (Section 5.1) belt/site reduction order is inverted. We could manage with this task if a more electronegative ion is inserted in the polar region substituting the original addenda metals. Vanadium (in the oxidation state 5+) or molybdenum (VI) are good candidates for this goal, and $P_2W_{15}V_3$ or $P_2W_{15}Mo_3$ are suitable anions for illustrating this phenomenon. In these two clusters, as the three substituting atoms occupy the three neighbouring polar sites of one α-PM_9 moiety, the point group of symmetry is formally reduced from D_{3h} to C_{3v}.

Analysis of $PW_{15}M_3$ derivatives

The first case in study is $P_2W_{15}V_3$. The structural changes introduced in this cluster are limited to the region of substitution. The V=O distances are about 1.65 Å, the bridging V–O–V bonds are 1.85 Å long, and the V–O–W about 1.98 Å. Thus, the shorter V–O–V bonds allow the vanadium centres to be closer, at only 3.24 Å. We may say that this tendency of localisation of the geometrical changes is general in HPAs. The outstanding characteristic of V^{5+} cations is their high affinity to *blue* electrons, especially compared to W^{6+} centres. As we showed for Keggin derivatives containing W and V, vanadium-centred MOs lower their energy and, in the present case, an inversion in the order of belt/cap d_{xy}-like orbitals occurs. The degenerate orbital of e symmetry (e' in the single-addenda species) turns out to be the LUMO in the V-substituted molecule. It is now fairly localised in the cap region with some contribution of the neighbouring belt of Ws. We provide a representation of this orbital in Figure 5.6.

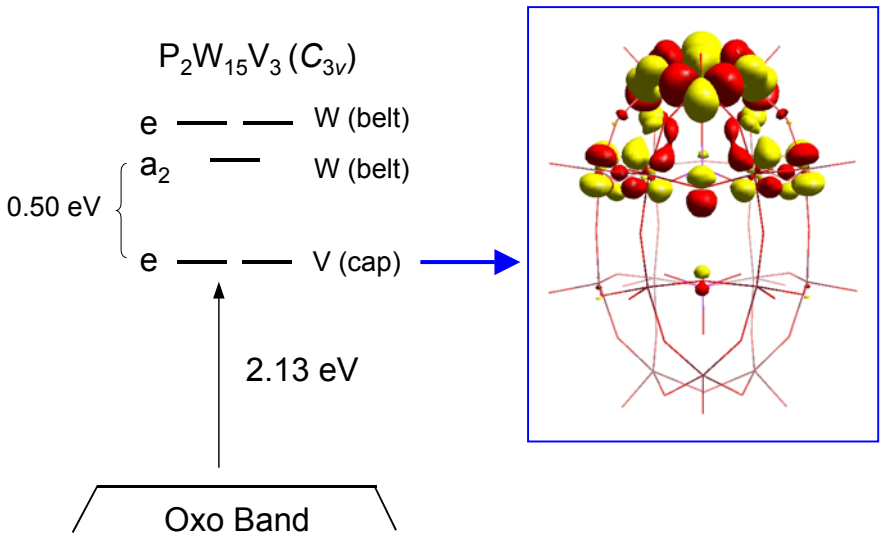

Figure 5.6. Scheme of the molecular orbitals for the V-substituted WD anion, α-$P_2W_{15}V_3$, and 3D representation of the LUMO.

Table 5.3. Percentile contributions of belt and cap metal centres to the LUMO, LUMO+1 and LUMO+2 for mixed-addenda WD anions.

Anion	*Sym*	*Belt*	*Cap*	*Belt*	*Cap*	*Belt*	*Cap*
		LUMO		LUMO+1		LUMO+2	
$P_2W_{15}V_3$	C_{3v}	13	60	65	0	55	10
$P_2W_{15}Mo_3$	C_{3v}	70	2	55	15	49	19
$P_2W_{15}Nb_3$	C_{3v}	66	0	61	7	51	16
$P_2Mo_{15}V_3$	C_{3v}	36	33	59	0	39	26
$P_2Mo_{15}Nb_3$	C_{3v}	60	0	63	3	57	5

Furthermore, it appears well-separated (0.50 eV at the DFT level) from the next two orbitals of a_2 and e symmetry, which are mainly d-W (belt) orbitals (schematic diagram in Figure 5.6). According to this orbital ordering, the first reduction would happen in vanadium cap orbitals and the energy difference between the two site reductions ($^2E - {}^2A_2$) was found to be 0.33 eV. The spin polarisation for the ^2E ground state of $P_2W_{15}V_31e$ confirms that the additional electron is essentially localised on the vanadium centres (Table 5.3), although some residence of the metallic electron is possible over the upper belt of tungstens. We did not study the introduction of V in the equatorial positions. In such a case, the LUMO would be a vanadium orbital with even a larger energy gap between it and the first W-centred MO, since the most electronegative *element* is in the most electronegative *site* (belt). Thus, the first reduction may take place in the belt sites and the difference between the belt and cap reduction would be larger than in the case we studied here. All these results are consistent with the studies of Pope and co-workers, who used cyclic voltammograms to find that the most positive cathodic peak for $P_2W_{17}V$ appears when the vanadium occupies a belt site.[6] The ESR spectra of anions substituted solely at the polar sites, $P_2V^{IV}V^{V}W_{16}$ and $P_2V^{IV}V_2{}^{V}W_{15}$ show that the vanadium centres really trap the metallic electron.[17] Now, two factors —the *most favourable belt position* and the *higher electronegativity* of the V^V ion— strongly compete to capture the additional electron.

Table 5.4. Spin polarisation ($\alpha - \beta$) and relative energies (in eV) for the two lowest states in several reduced mixed-addenda WD anions.

	Sym	($\alpha - \beta$)		*E*	($\alpha - \beta$)		*E*
		Belt	Cap		Belt	Cap	
		^{2}E			$^2A_2$		
$P_2W_{15}V_3$	C_{3v}	0.18	1.00	0.00	0.88	–0.011	0.33
$P_2W_{15}Mo_3$	C_{3v}	0.34	0.61	0.00	0.98	–0.03	–0.018
$P_2W_{15}Nb_3$	C_{3v}	0.87	0.095	0.00	0.90	–0.010	–0.14
$P_2Mo_{15}V_3$	C_{3v}	0.44	0.55	0.00	0.81	–0.020	0.18
$P_2Mo_{15}Nb_3$	C_{3v}	0.91	0.052	0.00	0.83	–0.015	–0.076

The second case of metal substitution studied here is that of $P_2W_{15}Mo_3$. Mo^{5+} is again more electronegative than tungsten(VI), although a priori less than vanadium(V). In this case only slight changes are introduced to the electronic structure. As a matter of fact, no inversion is found in the first three (and more relevant) Kohn–Sham molecular orbitals. The LUMO is still an a_2 belt-centred orbital, with only 2% of d-Mo orbitals. Just above in energy appear two degenerate e orbitals with some contribution of Mo: 15% and 19% for LUMO+1 and LUMO+2, respectively. This means that there is some contribution of cap-metals in both e orbitals. Even though, these contributions are all modest, showing that Mo is notably less electronegative than V in metal-oxide frameworks. So, the polar Mo_3O_{13} triad is not expected to accept the first metallic electron since the equatorial Ws are still in advantage for it. In Table 5.3 are shown the percentile contributions and, in Table 5.4, the spin populations of some states of interest concerning the single-reduced system. The reader may notice that the $^2A_2$ state is slightly more stable; at any rate, as the MO show, a strong competition between this and the ^{2}E" occurs since the LUMO and the next orbital are almost degenerate. A schematic diagram of the levels of energy in the $P_2W_{15}M_3$ WD anions computed is in Figure 5.7.

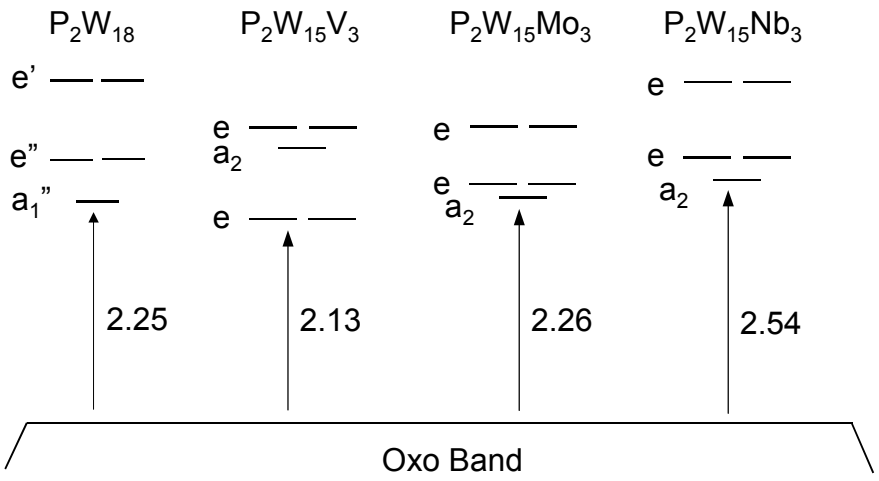

Figure 5.7. Schematic diagram of the frontier orbitals for the series of $P_2W_{15}M_3$ anions computed, with M = V, Mo and Nb. The H-L gaps are represented in eV for comparison.

The third tungsto-derivative studied is $P_2W_{15}Nb_3$. This derivative has the particularity that contains niobium(V), which is known to be less electronegative than W in its highest oxidation state. Probably the novel feature introduced by Nb in this set of WD anions is that the H-L gap is bigger than the parent P_2W_{18} form by 0.3 eV. Although the LUMO is absolutely centred on the belt Ws (66% W, 0% Nb), the presence of Nb in the polar region is more than tangible. We may expect that the oxidising power is decreased when Nb replaces W. The homologous $P_2Mo_{15}Nb_3$ is expected to behave similarly since Nb occupies the cap region and the most EN element is Mo.

One case of special interest is the vanadomolybdate, $P_2Mo_{15}V_3$, where there is a considerable competition between vanadium and molybdenum for the extra electrons. The most electronegative centre occupies the least favoured position in front of reduction and *vice versa*. As Table 5.3 shows, the LUMO of e symmetry in $P_2Mo_{15}V_3$ is not localised in one of the regions of the molecule and the participation of belt Mo (36 %) and cap V (33 %) orbitals is similar. The next metallic orbital of a_2 symmetry is only separated from the LUMO by 0.19 eV and is basically a belt orbital (59 %). This competition between Mo and V orbitals yields a spin density distribution in

the reduced complex of 0.55 e for cap V atoms and 0.44 e for belt Mo atoms. The energy difference between the two states ^2E and $^2A_2$ was computed to be only 0.18 eV. This competition is still more important in $P_2W_{15}Mo_3$ since those two states associated to the first reduction in cap (^2E) and belt ($^2A_2$) sites were found degenerate, result that does not fully match with the fact that the first reductions in $P_2W_{15}Mo_3$ are restricted to the Mo centres.[18-19] Although the origin of this discrepancy is unclear, we believe that present DFT calculations probably exaggerate the energy gap between cap and belt reductions for a given metal. We provide molecular orbital diagrams in Figure 5.8 the mixed-addenda WD systems derived from the 2:18 molybdate, in which three neighbouring capping octahedra were substituted.

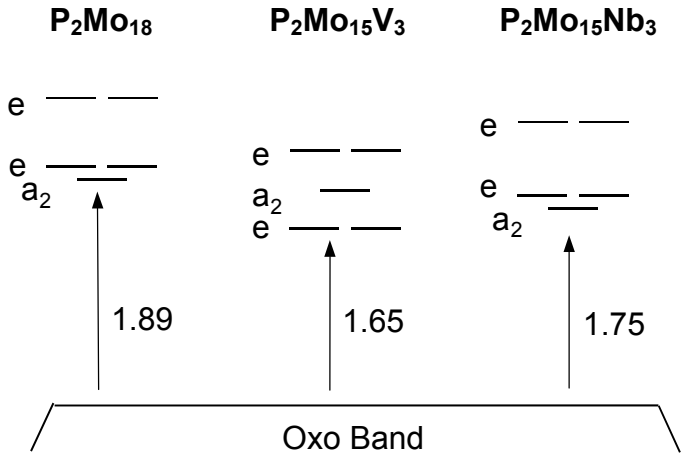

Figure 5.8. Schematic diagram of the frontier orbitals for the series of $P_2Mo_{15}M_3$ anions computed, with M = V and Nb. The H-L gaps are represented in eV.

5.3. Study of the Relative Stability of α/β-Wells–Dawson Anions

Introduction

The comprehension of the rotational isomerism occurring in some heteropolyanions is of great interest for the understanding and the applications of POMs. Although the relative instability of β isomers compared to α be accepted as a general rule, recent experimental and theoretical studies have shown that the differences in stability between the two isomers may be quite small.[20] In chapter 4 we made a detailed analysis of the factors that govern the relative stability of the α and β isomers of the Keggin anion, $[XM_{12}O_{40}]^{n-}$, with M = W, Mo and X a main group element.[8] The α isomer has T_d symmetry and the β isomer, of C_{3v} symmetry is derived from a 60º rotation of one M_3O_{13} triad about a three-fold axis of the α form (Figure 4.1).[21] DFT calculations also showed that the metallic (*blue*) electrons incorporated in the $M_{12}O_{36}$ framework and the greater stability of the β isomer are closely related. This gain in stability of the β isomer may be because there is a reduction in symmetry when going from α to β and a subsequent decrease in the energy of the LUMO. The rotational isomerism of Keggin structures also takes place in WD heteropolyanions. Pope, in the middle 60's,[6] and Contant's group[22] explored the electrochemistry of X_2M_{18} and mixed-addenda derivatives. They found that β anions also gain electrons at more positive potentials than the α forms although the difference is smaller than in α/β-Keggin pairs. Here we extend the previous study of section 5.1 on α-WD heteropolyanions[12] to analyse the α/β isomerism in WD structures. In particular, we focus on the relative stability of these isomers for $[P_2Mo_{18}O_{62}]^{6-}$, $[P_2W_{18}O_{62}]^{6-}$ and $[P_2W_{15}V_3O_{62}]^{9-}$, as well as the effect of the reduction processes on this equilibrium. The redox properties of the α isomer of WD structures were presented in sections 5.1-2. For the β isomer, we can conduct the same procedure to explore the reduction energies. As well as the Keggin anion, WD heteropolyanions can undergo structural isomerisations. If instead of two A-α-PW_9 moieties to give the α-P_2W_{18} framework we formally put together one A-α- and one A-β-PW_9 form, the result is the β-P_2W_{18} anion. This is characterised by having one α- and one β-Keggin-like half. In addition, it exists another isomeric

form, the so-called γ-P_2W_{18}. In this case, both PW_9 subunits are A-β forms. They are not discussed here.

Structure of $P_2W_{15}M_3$ anions

Geometry optimisations performed on the α and β[21,23] isomers of the title anions led to the structures listed below. The α isomer of P_2W_{18} was computed under the constraints of D_{3h} symmetry group whereas, for the corresponding β isomer, the symmetry of the molecule is C_{3v} (representations in Figure 5.9). The reader shall see below that the analogous molybdates have less symmetry.

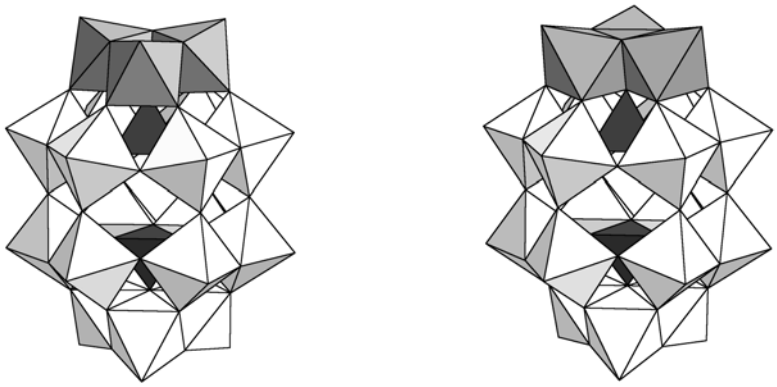

α-$P_2W_{15}M_3$ (D_{3h}) **β-$P_2W_{15}M_3$** (C_{3v})

Figure 5.9. Polyhedral representation of α- and β-$P_2W_{15}M_3$. A 60º rotation of one of the polar triads (shaded) about the vertical three-fold axis of symmetry of the alpha form leads to the beta one.

As it was already commented above, the geometries of the heteropolyanions are very well reproduced at the present level of theory. The largest discrepancy always appears in the W–O_{term} oxygen bonds, which are systematically underestimated by an average of 0.05 Å.[2,4] Deviations in the terminal bonds should not modify the reduction properties discussed here since they would essentially affect the energy of the d_{xz}- and d_{yz}-type orbitals, which are not the lowest. The reader will notice from Table

5.5 that the geometrical differences between isomers of the same formula are very small. Only the $M_b–O_{b3}–M_b$ angle appears to be always 4–5º bigger in the β form.

Table 5.5. Computed angles (in degrees) and interatomic distances (in Å) for a series of fully oxidised α and β Wells–Dawson anions. See Figure 5.1 for the labelling of metal and oxygen sites.

Anion (Sym.)	$M_c–O_{term}$	$M_c–O_{b1}$	$M_c–O_{b2}$	$M_b–O_{b2}$
α-P_2W_{18} (D_{3h})	1.74–1.75	1.94	1.90	1.95
β-P_2W_{18} (C_{3v})	1.74–1.75	1.94	1.90	1.95
α-P_2Mo_{18} (D_3)	1.74	1.89–2.04	1.84–2.05	1.85–2.12
β-P_2Mo_{18} (C_3)[a]	1.74–1.75	1.88–2.05	1.84–2.05	1.86–2.12
α-$P_2W_{15}V_3$ (C_{3v})	1.76–1.77 (W) 1.65 (V)	1.96 (W) 1.85 (V)	1.89 (W) 1.98 (V)	2.01 (W) 1.84 (V)
β- $P_2W_{15}V_3$ (C_{3v})	1.76–1.77 (W) 1.65 (V)	1.96 (W) 1.84 (V)	1.89 (W) 1.98 (V)	2.01 (W) 1.84 (V)

Anion (Sym.)	$M_c–M_c$	$M_b–M_b$[a]	$M_b–O_{b3}–M_b$
α-P_2W_{18} (D_{3h})	3.42	3.70 3.76	163º
β-P_2W_{18} (C_{3v})	3.41–3.42	3.69–3.74 3.78	166º
α-P_2Mo_{18} (D_3)	3.46	3.42–3.74 3.89	163º
β-P_2Mo_{18} (C_3)[b]	3.45–3.47	3.40–3.78 3.88	167–169º
α-$P_2W_{15}V_3$ (C_{3v})	3.46 (W) 3.24 (V)	3.62–3.73 3.84	164º
β- $P_2W_{15}V_3$ (C_{3v})	3.46 (W) 3.25 (V)	3.31–3.41 3.85	168º

a) β-P_2Mo_{18} was optimised without symmetry constraints

b) First values concern two metals on the same belt, whereas the second number is the distance between two metals of different belts.

The substitution of three neighbouring tungsten atoms by vanadiums in one of the polar triads induces some structural changes restricted to the replaced octahedrons. Typically, all the V–O bonds are shorter than the homologous W–O. As a consequence, the V···V distances in the substituted triad are also shorter (3.24 Å) than the typical W···W separation (3.42 Å).

Electronic properties

The discussion of the α/β isomerism in WD clusters might be introduced with regard to that of the Keggin anion. In a first step, a qualitative study of the electronic structure can be of help for understanding their redox properties. Let us show a correlation diagram of the frontier orbitals for the most and least symmetric PW_{12} and P_2W_{18} isomers (Figure 5.10).

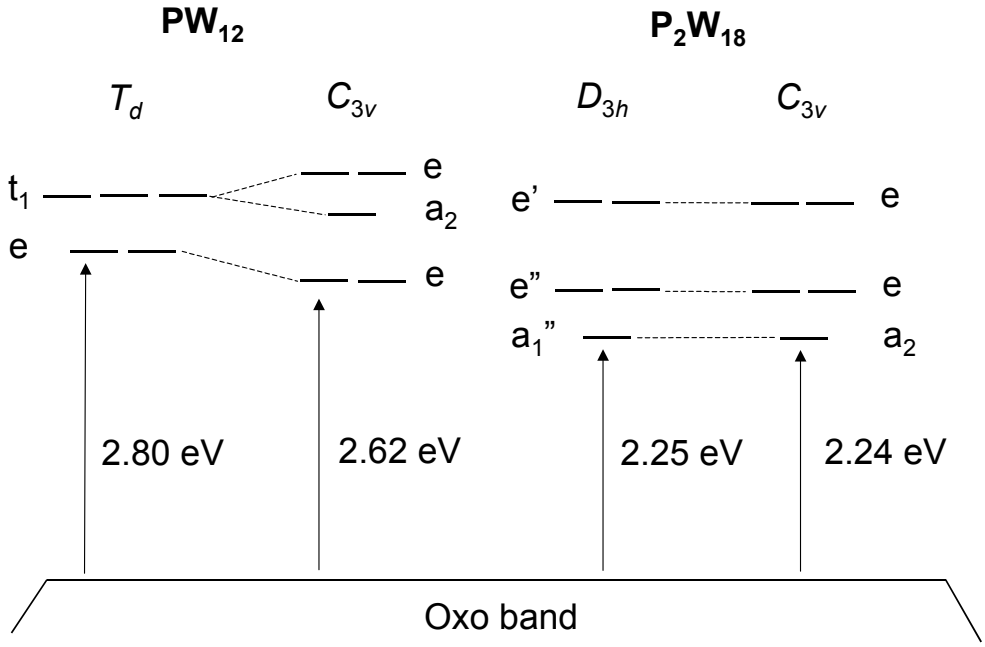

Figure 5.10. Relative energies of the lowest metallic orbitals of the α and β isomers of PW_{12} and P_2W_{18} anions.

The frontier orbitals e and t_1 (LUMO and LUMO+1, respectively) of the α-Keggin split into e and e + a_2 after one W_3O_{13} triad is rotated in the T_d structure to give the β isomer. Mixing the orbitals of the same symmetry leads to a decrease in the H-L gap from 2.80 eV in the T_d geometry to 2.62 eV in the C_{3v} geometry. Consequently, the β forms are always more easily reduced than the corresponding α forms. The formal substitution of three octahedrons in α-XM_{12} anions by a XM_9 unit (to give the WD anion) breaks the equivalence of all metals and two types of metal ions appear in an α-X_2M_{18} framework. Cap and belt metals do not participate in the lowest unoccupied orbitals equally. Whereas the d_{xy} orbitals centred on the twelve *belt* metals are the major contributors to the LUMO (a_1") and LUMO+1 (e"), the LUMO+2 (e') is mainly composed of d_{xy} orbitals centred on the six cap metals. According to this orbital composition, the first reduction in the WD anions takes place in the belt region. The 3D representation of the LUMO is given in Figure 5.11.

From Figure 5.10, it arises that the energy of WD anion frontier orbitals do not change significantly when one of the cap triads is rotated and, therefore, the redox properties of β-P_2W_{18} are expected to be similar to those of the α isomer. By studying the reduced species we can confirm the predictions made from molecular orbital analysis of the oxidised anions. If n is the number of blue electrons in the lowest metallic orbital (a_1" and a_2 for the D_{3h} and C_{3v} isomers, respectively), the energy difference between the isomers hardly changes with n. The magnitude $\Delta E_{\beta-\alpha}$ is 1.83 kcal mol^{-1} for n = 0 and decreases by only 0.13 kcal mol^{-1} for n = 1 and 0.72 kcal mol^{-1} for n = 2. These positive values for $\Delta E_{\beta-\alpha}$ clearly indicate that the α isomer is the most stable but the difference in stability between the two isomers is quite small. The relative thermodynamic stabilities of the α and β of $[P_2W_{18}O_{62}]^{6-}$ were recently established both in solid state by differential scanning calorimetry and in solution by ^{31}P NMR.[24] Both techniques give that the α isomer is more stable than the β one by ~4 kcal mol^{-1}. Taking into account that the theoretical calculations were carried out with the isolated anions the agreement between experimental and theoretical results can be considered excellent.

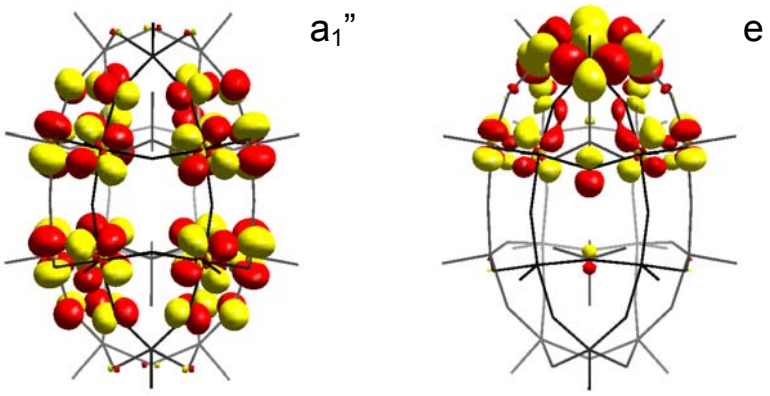

Figure 5.11. 3D representations for the LUMO of α-$[P_2W_{18}O_{62}]^{6-}$ (orbital of a_1” symmetry delocalised over the belt metal atoms) and α-$[P_2W_{15}V_3O_{62}]^{9-}$ (one of the components of the e symmetry orbital centred at the vanadium cap ions).

We presented above the characteristics of the molybdate WD anions. The α structure is quite well studied by means of different techniques but, to our knowledge, there is no experimental evidence about the shape of the β isomer. Perhaps the most significant data concerns its reduction properties, which are quite similar to those of the α counterpart.[6b] For the β isomer, two structures were explored: a non-distorted C_{3v} structure, similar to the one optimised for β-P_2W_{18}, and a structure with alternate Mo–O bonds of C_3 symmetry (Figure 5.12). Considerable computational effort was made to optimise the latter because the C_3 point group is not available in the ADF package, and the geometry had to be optimised without symmetry constraints. As in the α isomer, the structure with an alternate arrangement of the Mo–O bonds is clearly more stable than the most symmetric form. The energy difference between the C_3 and C_{3v} structures is 8.2 kcal mol^{-1}. Also as in the α isomer, the Mo–O distances are between 1.83 and 2.12 Å. These relatively important energies strongly suggest that the two α and β forms of P_2Mo_{18} have similar structures, with series of short and long Mo–O bonds. We looked for a possible chiral structure for the α-2:18 tungstate, however, the optimisation process always yield the most symmetric D_{3h} form. This finding seems in agreement with the observation of chiral structures only in molybdates.[10-11]

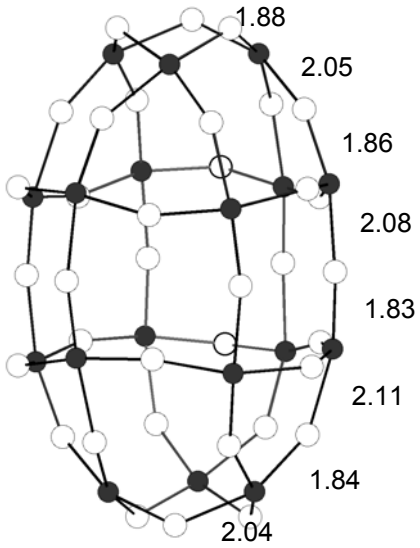

Figure 5.12. Ball-and-stick view of the DFT computed geometry of the β-P_2Mo_{18} anion with formal C_3 symmetry. White and black spheres represent oxygen and molybdenum atoms, respectively. The two internal PO_4 units, as well as the terminal oxygens, are not included for clarity. The distances (in Å) highlight the alternative disposition of long and short Mo–O bonds forming three interpenetrating loops.

If a more electronegative ion, like V^{5+}, is incorporated into a polar site, there is an inversion of the traditional belt/cap site reduction order. We analysed the effect that the reduction may have on the equilibrium of the α/β-$P_2W_{15}V_3$ species, where the three Vs occupy three sites in the same triad (shaded octahedrons in Figure 5.9). The substitution of W by the more electronegative V inverts the order of belt/cap d_{xy}-like orbitals and then the LUMO in $P_2W_{15}V_3$ is an orbital of e symmetry mainly centred on the three equivalent vanadium atoms[17] (60% V orbitals – 10% belt W orbitals, Figure 5.11). The LUMO+1 is composed of 65% belt tungsten orbitals and the LUMO+2 of 48% belt W and 10% V orbitals. The shape and energy of the β-form orbitals resemble those of the α-form orbitals. The H-L gap is similar in both structures. This is important because although the substitution reduces a metal ion directly involved in the rotation, it does not significantly alter the α/β equilibrium in WD anions. As the values in Table

5.6 show, the computed $\Delta E_{\beta-\alpha}$ are only slightly higher than those found for the non-substituted P_2W_{18} cluster. Moreover, the effect of the single reduction on the α/β equilibrium in $P_2W_{15}V_3$ does not exceed the 0.5 kcal mol^{-1}.

Table 5.6. Experimental reduction potentials and calculated relative stabilities for several heteropolyanions.

	Reduction Potentials[a] *(in V)*		
Compound	α	β	$\Delta V_{\beta-\alpha}$
Keggin			
AlW_{12}	–0.62 (1)	–0.45 (1)	0.17
SiW_{12}	–0.26 (1)	–0.14 (1)	0.12
PMo_{12}	+0.36 (2)	+0.55 (2)	0.19
Wells–Dawson			
P_2W_{18}	+0.045 (1)	+0.059 (1)	0.014
P_2Mo_{18}	+0.46 (2)	+0.53 (2)	0.07
	$\Delta E_{\beta-\alpha}$ *(in kcal* mol^{-1}*)* [b]		
	$n = 0$ [c]	$n = 1$ [c]	$n = 2$ [c]
Keggin			
PW_{12}	+6.46	+3.00	+0.92
SiW_{12}	+6.00	+2.54	–3.30
PMo_{12}	+4.84	+1.49	–2.59
Wells–Dawson			
P_2W_{18}	+1.83	+1.70	+1.11
P_2Mo_{18}	+2.92	-	+0.60
$P_2W_{15}V_3$	+2.54	+2.03	+2.31

a) Values in parentheses are the number of metallic electrons added
b) Positive values for $\Delta E_{\beta-\alpha}$ mean that the α isomer is the most stable
c) Number of metal or blue electrons in the framework

For the α/β equilibrium in 2:18 molybdates, we found an energy difference of 2.9 kcal mol^{-1} between the fully oxidised forms. This is

smaller than the difference computed for PMo_{12} (4.8 kcal mol^{-1}) and PW_{12} (6.5 kcal mol^{-1}), but somewhat larger than the one found for P_2W_{18} (1.8 kcal mol^{-1}). The LUMO in the chiral α (D_3) isomer of P_2Mo_{18} is 1.86 eV above the oxygen band. The 60º rotation of one capping triad decreases the energy of the LUMO by 0.17 eV, whereas the same transformation in the D_{3h} structure of P_2W_{18} reduces the stabilisation of the LUMO to a mere 0.01 eV. This reduction favours the stability of the β form. Hence, after the second reduction, the C_3 structure is only 0.60 kcal mol^{-1} less stable than the D_3 one. The relative stability of α and β isomers fully agrees with the reduction potentials given in Table 2. In general, the β isomers reduce at more positive potentials than the α counterparts, and this behaviour is much more significant in the most symmetric Keggin frameworks than in the WD anions. For these latter anions, the polarographic data suggest that the gain in stability of the β form due to the reduction is somewhat larger for molybdates than tungstates.[6]

References and Notes

[1] Wells, A. F. *Structural Inorganic Chemistry*. Clarendon Press. Oxford, U. K., 1945.

[2] Dawson, B. *Acta Crystallogr., Sect. B*. **1953**, *6*, 113.

[3] Strandberg, R. *Acta Chem. Scand., Ser. A.* **1975**, *29*, 350.

[4] D'Amour, H. *Acta Cryst., Sect C.* **1976**, *32*, 729.

[5] Day, V. W.; Klemperer, W. G. *Science.* **1985**, *228*, 533.

[6] (a) Pope, M. T.; Papaconstantinou, E. *Inorg. Chem.* **1967**, *6*, 1147. (b) Papaconstantinou, E.; Pope, M. T. *Inorg. Chem.* **1967**, *6*, 1152. (c) Varga, G. M.; Papaconstantinou, E.; Pope, M. T. *Inorg. Chem.* **1970**, *9*, 662. (d) Papaconstantinou, E.; Pope, M. T. *Inorg. Chem.* **1970**, *9*, 667.

[7] López, X.; Maestre, J. M.; Bo, C.; Poblet, J. M. *J. Am. Chem. Soc.* **2001**, *123*, 9571–9576.

[8] Maestre, J. M.; López, X.; Bo, C.; Casañ-Pastor, N.; Poblet, J. M. *J. Am. Chem. Soc.* **2001**, *123*, 3749–3758.

[9] Kazanskii, L. P.; Fedotov, M. A. *J. Chem. Soc., Chem. Commun*. **1980**, 644.

[10] Pope, M. T. *Inorg. Chem.* **1976**, *15*, 2008.

[11] Garvey, J. F.; Pope, M. T. *Inorg. Chem.* **1978**, *17*, 1115.

[12] López, X.; Bo, C.; Poblet, J. M. *J. Am. Chem. Soc.* **2002**, *124*, 12574.

[13] Kozik, M.; Baker, L. C. W. *J. Am. Chem. Soc.* **1987**, *109,* 3159. Casañ-Pastor, N.; Baker, L. C. W. *J. Am. Chem. Soc.* **1992**, *114,* 10384 and references therein.

[14] Suaud, N; Gaita-Ariño, A.; Clemente-Juan, J. M.; Sánchez-Marín, J.; Coronado, E. *J. Am. Chem. Soc.* **2002**, *124,* 15134.

[15] Borrás-Almenar, J. J.; Clemente-Juan, J. M.; Coronado, E.; Tsukerblat, B. S. *Chem. Phys.*, 1995, **195**, 1.

[16] Borshch, S. A.; Bigot, B.; *Chem. Phys. Lett.* **1993**, *212*, 398.

[17] Harmalker, S. P.; Pope, M. T. *J. Am. Chem. Soc.* **1981**, *103*, 7381–7383.

[18] Kozik, M.; Hammer, C. F.; Baker, L. C. W. *J. Am. Chem. Soc.* **1986**, *108,* 2748. *ibid.* **1986**, *108*, 7627.

[19] Kozik, M.; Baker, L. C. W. *J. Am. Chem. Soc.* **1990**, *112,* 7604.

[20] Weinstock, I. A.: Cowan, J. J.; Barbuzzi, E. M. G.; Zeng, H.; Hill, C. L. *J. Am. Chem. Soc.* **1999**, *121*, 4608.

[21] Baker, L. C. W.; Figgis, J. S. *J. Am. Chem. Soc.* **1970**, *92*, 3794.

[22] Some recent publications are: Keita, B.; Belhouari, A.; Nadjo, L.; Contant, R. *J. Electroanal. Chem.* **1998**, *442*, 49. Keita, B.; Girard, F.; Nadjo, L.; Contant, R.; Canny, J.; Richet, M. *J. Electroanal. Chem.* **1999**, *478*, 76. Keita, B.; Lu, Y. W.; Nadjo, L.; Contant, R.; Abbessi, M.; Canny, J.; Richet, M. *J. Electroanal. Chem.* **1999**, *477*, 146. Contant, R.; Abbessi, M.; Canny, J.; Richet, M.; Keita, B.; Belhouari, A.; Nadjo, L. *Eur. J. Inorg. Chem.* **2000**, 567. Keita, B.; Lu, Y. W.; Nadjo, L.; Contant, R. *Eur. J. Inorg. Chem.* **2000**, 2463.

[23] Acerete, R.; Harmalker, S.; Hammer, C. F.; Pope, M. T.; Baker, L. C. W. *J. Chem. Soc., Chem. Commun.* **1979**, 777. Massart, R.; Contant, R.; Fruchart, J. M.; Ciabrini, J. P. Fournier, M. *Inorg. Chem.* **1977**, *16*, 2916.

[24] Anderson, T. M.; Hill, C. L. *Inorg. Chem.* **2002**, *41*, 4252.